Title

Calibrating SLEUTH with big data: Projecting California's land use to 2100

Authors

Clarke, Keith C

Johnson, J Michael

Publication Date

2020-09-01

DOI

10.1016/j.compenvurbsys.2020.101525

Peer reviewed

Computers, Environment and Urban Systems 83 (2020) 101525

Contents lists available at ScienceDirect

Computers, Environment and Urban Systems

journal homepage: www.elsevier.com/locate/ceus

Calibrating SLEUTH with big data: Projecting California's land use to 2100

Keith C. Clarke*, J. Michael Johnson

Department of Geography, University of California, Santa Barbara, Santa Barbara, CA 93106-4060, United States of America

ARTICLE INFO

Keywords:
Land use
Land cover change
SLEUTH
California
Calibration
Simulation

ABSTRACT

This study investigated the spatial consistency of the SLEUTH urban growth and land use change model using a massive data set. The research asks whether SLEUTH can yield both a reliable forecast of land use in the state of California for the year 2100 CE, and an assessment of the forecast's reliability. Data were prepared, and SLEUTH calibrated for 174 tiles made by partitioning the data within the 6 California State Plane Zones. A null hypothesis that all data divisions of California would give similar calibration outcomes so that a uniform simulated rate of growth would apply to statewide future simulations was proven false by mapping and Moran's I values. Spatial autocorrelation was found to propagate forward into the SLEUTH forecasts, resulting in major differences within the state in land use change and change rates. We also explored the spatial distribution of the rules that changed pixels between land use classes, finding that almost 99% of forecast growth in California comes from outward spread from new and existing settlements. The paper concludes with an examination of the uncertainty inherent within, and displayed by the SLEUTH forecasts.

1. Introduction

Land use change is a principal driver of global change, and among all land use transitions, the spread of urban areas has a dominant negative impact on greenhouse gas emissions, loss of natural space, farmland and biodiversity, along with increased congestion and environmental pollution (Foley, DeFries, Asner, Barford, et al., 2005). The mapping, modeling, and forecasting of these changes are of critical concern for anticipating and mitigating these negative consequences. Among the most popular and successful land use change models are those based on cellular automata (Clarke, 2019). SLEUTH is a mature land use change and urban growth cellular automaton simulation model that ingests gridded data, and creates probabilistic simulations of future land use states (Chaudhuri & Clarke, 2013). The cellular automaton embeds rules governing urban growth based on spread rules, and class-to-class land use changes based on a Markovian transition matrix computed from past changes. Modeling consists of preparing the input data, testing the model code, using past data to calibrate the model's behavioral coefficients, and allowing the model to run into the future to create scenarios of growth and change. Traditionally, the calibration sequence consisted of a brute force method that adjusted the coefficients to best fit the prior data (Silva & Clarke, 2002). However, this brute force method is both labor and CPU intensive, which has proven to be a barrier to the model's application.

As such, the SLEUTH calibration process has been studied in detail (Clarke, 2008; Clarke, Hoppen, & Gaydos, 1996). Several studies explored the use of parallel and high-performance computing to decrease the calibration time (Chaudhuri & Foley, 2019; Guan & Clarke, 2010). Others investigated the sensitivity of the model to the number of Monte Carlo iterations used (Goldstein, Dietzel, & Clarke, 2005); the duration used for calibration and forecasting (Peiman & Clarke, 2014); the changes made by the self-modification rules (Saxena & Jat, 2018); the means of including past and future exclusions (Akin, Clarke, & Berberoglu, 2014; Onsted & Clarke, 2012); and the use of alternative goodness of fit measures, such as landscape metrics (Herold, Couclelis, & Clarke, 2005). Sakieh, Salmanmahiny, and Mirkarimi (2016) tested alternative models against SLEUTH, such as logistic regression and a multi-layer perceptron. Dietzel and Clarke (2005) explored the scale effect of disaggregating land use classes on model calibration and forecasts, while Jantz and Goetz (2005) explored the impact of scale geographically.

Significant changes to SLEUTH calibration involved the analysis of model behavior to detect correlation among the original 13 fit metrics, which resulted in a subset of 8 being used for the Optimal SLEUTH metric (Dietzel & Clarke, 2007). Other work offered new versions of the model with different means of calibration (Jantz, Drzyzga, & Maret, 2014: CAGIS, 2019; Jantz, Goetz, Donato, & Claggett, 2010; Houet, Aguejdad, Doukari, Battaia, & Clarke, 2016). Liu, Sun, Yang, Su, and Qi (2012) made two modifications to improve SLEUTH: using ant colony optimization to calibrate and performing sub-regional calibration to

* Corresponding author.
E-mail addresses: kcclarke@ucsb.edu (K.C. Clarke), mike.johnson@geog.ucsb.edu (J.M. Johnson).

https://doi.org/10.1016/j.compenvurbsys.2020.101525
Received 21 April 2020; Received in revised form 7 July 2020; Accepted 8 July 2020

replace calibration of the entire study area. Both modifications improved the calibration accuracy and efficiency compared with the original SLEUTH applications. Wu et al. (2009) employed the relative operating characteristic (ROC) curve statistic, multiple-resolution error budget, and landscape metrics for comparison and validation to evaluate the simulation performance of the SLEUTH urban growth model in the Shenyang metropolitan area of China.

Probably the most significant improvement for SLEUTH calibration was the conversion of the calibration method from brute force to a genetic algorithm. After initial experiments with the new method (SLEUTH-GA) (Clarke-Lauer & Clarke, 2011), a more complete set of procedures and constants were derived for more general application and the code added to the SLEUTH website (Clarke, 2017; Clarke, 2018). Testing showed that SLEUTH-GA could calibrate the model with a computational speed-up of between 3 and 22 times. This means that a single city or regional data set can be calibrated in days instead of years. Jafarnezhad, Salmanmahiny, and Sakieh (2015) also showed the advantages of the genetic algorithm, which include fully automating the calibration process and removing any remaining human subjective choice.

Zhou, Varquez, and Kanda (2019) used the historical distribution of global population as a proxy for urban land cover, to calibrate SLEUTH for the period 2000 to 2013. This simulation used two urban growth layers as 50 arc-minute grids to simulate global urban cover, which they forecast to reach 1.7×10^6 km^2 by 2050. The modeling used partitioned data (tiles) and repeat applications by region to get global extent. To reduce the computational load in the calibration, not all coefficients were varied, and data tiles with less than about 25 km^2 of urban area according to the 2012 global urban map were excluded. The 2012 global urban extent data were averaged from Landscan data for 2012 and 2013 (Oak Ridge National Laboratory, 2020). Data partitioning also enabled SLEUTH application for other massive data sets, for example all of Italy (Martellozzo, Amato, Murgante, & Clarke, 2018). With these developments, SLEUTH has gained the ability to not only deal with big data, but to ensure accurate and timely calibration even with massive extents and high resolution.

In the present study we took advantage of these SLEUTH improvements to simulate the State of California for the entire 21st century. In addition, we used a very high spatial resolution (30 m) for which data were available. The purpose of the study is to investigate the consistency of SLEUTH spatially. Our research question is: can we create both a reliable forecast of land use in California (excluding the Channel Islands) for the year 2100 CE, and an assessment of the forecast's reliability? A null hypothesis is that all data divisions of California would give similar calibration outcomes (goodness of fit and coefficient values) so that a uniform simulated rate of growth will apply to future simulations. Failing this, is there spatial autocorrelation among the calibrated values? Finally we explored the spatial distribution of the rules that govern land use changes, and the uncertainty inherent within them, as revealed by the SLEUTH model.

2. Compiling the data

SLEUTH requires data for slope, land use, exclusions, urban extent, transportation and hillshade, where the last is used for visualization and not a part of the model. Percent slope and hillshade were calculated from the 1 arc *sec* elevation data in the USGS National Elevation Dataset. California Land Use was extracted from the National Land Cover 30 m data for 2001, 2006, and 2011, derived from Landsat satellite data as part of the Multi-Resolution Land Characterization (MRLC) project (See: https://www.mrlc.gov/about). Land use class labels were abbreviated into 13 classes, and followed the MRLC classification but without the classes specific to Alaska. Finally, all urban classes (and densities) were compressed into a single class. For the modeling, 2001 was assigned as the initial year and the 2011 layer duplicated for 2017, as at the time no newer land use data were available. Exclusions came from the 2017 GreenInfo Network California Protected Areas Database, the 2016 GreenInfo Network California Conservation Easement Database, the GreenInfo Network Military Lands, and the GreenInfo Network Tribal Lands (BIA). Lastly, water body exclusions came from the National Hydrography Dataset Plus V2. Exclusion values in this layer vary between 0 and 100, with 0 meaning no resistance to urbanization and 100 meaning complete exclusion. Values were assigned subjectively by exclusion category and land use classification.

Urban extents were extracted from the USDA Cropland Dataset between 2007 and 2015, and from the 2001, 2006 and 2011 NLCD land use layers. Starting in 2001, these data layers were forward overlain, so that any pixel urbanized in any time period remained urban in all future periods, assuming that any pixel deurbanized was a commission error. Since many of these layers added little data year to year, the dates of 2001, 2006, 2008, 2012, 2014 and 2017 were selected to reduce the computation time.

For transportation, the TIGER line files from the US Census were compiled for 2000, 2005, 2010, and 2015. The road designations were as reported by the US Department of Transportation, with four classes varying by definition over time. All features whose names started with “Interstate”, “State”, “Hwy”, “Fwy” or “Highway” were included. For 1990 to 2005, the Census Feature Class Codes were A10 to A18; for years 2010 to 2015, the MAF/TIGER Feature Classification Codes were S1100 and S1200. All maps were projected into the Albers equal area projection, to preserve the equal area property across the state and referenced to the NAD83 datum. Lastly, the data were partitioned into 8 subsets, corresponding with the 6 California State Plane Coordinate Zones.

3. Tiling

Each final data set contained 789,777,829 pixels, and since each model run used 6 urban layers, 3 roads layers, 2 land use layers, 1 exclusion, 1 slope and 1 hillshade layer, each model calibration used 14 times the data of the base rasters for a grand total of 1.1 × 10^10 pixels. The whole map was assembled as GeoTIFFs in the Albers equal area map projection at the Landsat native 30 m pixel size. The raster datasets were so large that the SLEUTH model was unable to allocate sufficient memory to execute. The data were then divided into 8 subsets corresponding with the extents of the State Plane Coordinate System zones for California (Fig. 1). Two zones (4 and 5) were still too large and were subsequently divided east/west into two zones apiece along county boundaries.

A second data partitioning used custom C language code to read each data set and partition it into 4 cells based on the bounding rectangle of the zone. Allowance was made for odd and even numbers of rows and columns. The quartering of tiles were then repeated

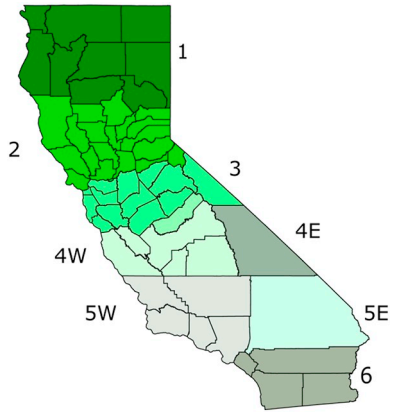

Fig. 1. Division of the California Data set into zones.

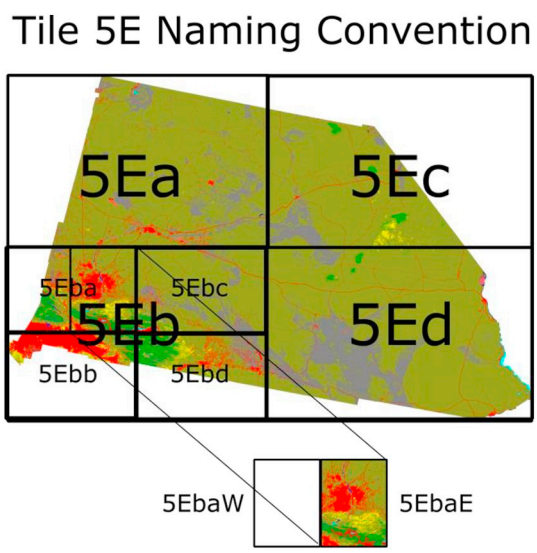

Fig. 2. Recursive Division of the Zones using a file naming convention. Example using Zone 5E (San Bernardino County). Sample tile has the label ca5EbaE. Eventually 174 such tiles were used for calibration and forecasting.

recursively, using the naming convention shown in Fig. 2. In four of the zones (ca1, ca4W, ca5E, ca5W) it was necessary to further divide the tiles by splitting them into east and west halves. The final data partitioning included 8 zones, four of them with 16 subtiles and four with 32 for a total of 192 subtiles. Eighteen of these fell outside the State Plane zones, had no data, or were in the ocean, leaving a calibration for 174 subtiles.

4. Executing the calibration

SLEUTH calibration uses scenario files that hold all needed file identification and parameter data for a SLEUTH model calibration run. Separate scenario files were prepared for each of the 8 major zones, and these were then modified manually to cycle through each of the subtiles. All input data for each zone was maintained in a separate folder in the 8-bit GIF format required by SLEUTH. Calibration consisted of invoking the SLEUTH-GA code using the Cygwin UNIX emulator for MS Windows. It was found that execution could be enhanced by using the "peflags –cygwin-heap" setting to increase the heap size and speed the execution. Having a GPU available (Intel Core i7-4770K at 3.5GHz and 4 GPU cores on an NVIDIA GeForce GPU) sped up the execution, nevertheless each calibration used 4 Monte Carlo iterations, took about 20 generations of the genetic algorithms with a genome size of 55, and ran for approximately 24 h, meaning that the full set of 174 calibrations used about a year of CPU time across two different computers. Results were output to a shell script file that called the clock at the start and end of each calibration run. Some typical results are shown in Table 1–of the five selected and different times, the tile average calibration took 28.32 h. Differences were due to the specifics of the task, how many tasks were running, the size of the tile, the amount of data it contained and the amount and complexity of the growth captured.

5. Calibration performance

The calibration period was 2001–2017, where the 2017 land use data was assumed unchanged from 2011. This assumption was needed to align the most current urban data (from USDA) with the land use data (from USGS), which were not available for 2017 at the time of the study (data for 2016 have subsequently become available). The results were explored first in terms of performance. An ideal model is able to replicate exactly the last calibration time period (2017) and all intermediate data sets, using only data from the start year (2001) and the land use transition matrix (2001–2017).

Much discussion has been made over how best to measure the accuracy or performance of a model calibration. We used five measures, the maximum and mean (over the chromosome) optimal SLEUTH metric (OSM) achieved, the producers and users accuracy, and the figure of merit (FOM). Producer's accuracy measures how often actual classes on the ground are correctly classed by the model, or its equivalent probability. The user's accuracy is referred to as reliability and is the complement of the Commission Error, i.e. 100% - Commission Error. It is calculated by taking the total number of correct classifications for a particular class and dividing it by the row total in the contingency matrix between the actual and the modeled end calibration year. The FOM is the ratio of the intersection of the observed change and the predicted change divided by the union of the observed change and predicted change. To compute this value, the persistence (i.e. a class remaining unchanged) was eliminated, and success or a "correct due to observed change predicted as change" set to only those cases where the pixel had changed class and the classes matched exactly. There is a bias when no or very few pixels change class, as getting the few changed pixels right can give perfect or near perfect performance. These measures are detailed extensively in Pontius Jr et al. (2007) and Table 2 outlines the descriptive statistics for the California SLEUTH calibration over the 174 subtiles.

Table 2 shows that the goodness of fit measures at the gene (Maximum OSM) and chromosome (Mean OSM) levels averaged 0.25146 and 0.17938, with medians of 0.21405 and 0.14654 respectively. The OSM metric is the product of 8 of the 13 SLEUTH metrics, each in the range {0–1.0}. The expected mean value of each of the 8 parameters, if they were identical, would be 0.842 and 0.787, and the medians 0.825 and 0.787 for the best gene and chromosome respectively. In fact, many of the fit parameters are close to 1.0, with only one or two of the fit measures lower. The independent measures of fit were computed for the 2001 land use layer matched to the simulated 2017 layer, using the 2017 actual layer as the reference map with custom C-code that read the SLEUTH data layers directly. This gave high values of the FOM (mean 0.9403, median 0.9786), producers accuracy (mean 0.9649, median 0.9883) and users accuracy (mean 0.9409 median 0.9794), indicating a successful calibration in all but a few subtiles.

However, the impressive mean and median statistics hide a large range in actual model performance. Fig. 3 is a boxplot of the data in Table 3, and clearly illustrates that the independent accuracy statistics are skewed high, while the two OSM measures are more normally distributed, but with more high outliers than low. These may be due to the many subtiles with little or no change, which the model did well in capturing. Figs. 4 and 5 show radar plots by subtile and by zone respectively, with values for the five performance metrics. These plots

Table 1
Sample calibration execution times and performance for five of the 174 subtiles.

Tile	Start time	End time	Calibration time (hours)	# Generations	Maximum OSM
5EbaE (Fig. 2)	Fri, Sep 20, 2019 8:54:12 AM	Sat, Sep 21, 2019 8:22:40 AM	23.47	20	0.009841
ca1ccW (best)	Mon, Sep 09, 2019 3:09:03 PM	Tue, Sep 10, 2019 3:27:46 AM	12.31	19	1.000000
ca5EcbW (median)	Wed, Sep 25, 2019 9:08:46 AM	Fri, Sep 27, 2019 2:06:34 AM	40.96	20	0.012062
ca4Ead (1st quartile)	Mon, Sep 9, 2019 11:48:47 AM	Tue, Sep 10, 2019 3:46:03 PM	27.95	20	0.081839
ca2dd (3rd quartile)	Thu, Sep 5, 2019 9:40:48 AM	Fri, Sep 6, 2019 10:35:37 PM	36.91	20	0.353441

Table 2
SLEUTH performance metrics for the 174 subtiles for the California data, over the calibration period 2001–2017.

	MaxOSM	MeanOSM	FOM	Producers Accuracy	Users Accuracy
Minimum	0	0	0.43824	0.60936	0.43824
Q1	0.08230	0.05560	0.94193	0.96715	0.94291
Median	0.21405	0.14654	0.97859	0.98834	0.97939
Q3	0.35299	0.26968	0.99687	0.99837	0.99689
Mean	0.25146	0.17938	0.94029	0.96489	0.94088
Maximum	1	0.71032	1	1	1

show the random nature of the differences in goodness of fit, with zone 2 performing best and zone 5 W performing worst, but with both high and low values occurring in all zones. Fig. 4 in particular hints at spatial autocorrelation in the metrics, as adjacent tiles are listed in order and show some degree of resembling their neighboring tiles in values.

Perhaps the most reliable performance measure is the maximum OSM, that achieved by the best performing gene within the chromosome at the end of the evolution of the genetic algorithm. As this is a composite measure, with mean and median values of 0.25146 and 0.21405, the expected individual measure values of 0.842 and 0.8250 are better indicators of actual proportion of model fit. The model's accuracy seems about equivalent to the usual measured accuracy of the land use classifications used as model input and are compatible with several other studies that have used the metric to measure calibration success.

6. Model behavior and parameters

The genetic algorithm creates an initial chromosome filled with random integer values in the {0…100} range. These are then changed in subsequent generations by cross over, competition, replacement, and mutation to evolve the final best fit parameters. Replacement ensures that new random genes can jump to the top and become the most fit at any time. The calibrations were run from a UNIX C-shell script as follows:

```
date > ../Output/CaliforniaZone6/DD/CAcal-DD
../grow.exe evolve scenario.ca6_calibrate 55 100 0.131600 55 50 > > ../Output/CaliforniaZone6/DD/CAcal-DD
date > > ../Output/CaliforniaZone6/DD/CAcal-DD
```

Table 3
Descriptive statistics for the five SLEUTH control parameters over the 174 subtiles, during the initial calibration phase.

	Diffusion	Spread	Breed	Slope	Road Gravity
Min	0.00	0.00	0.00	0.00	0.00
Q1	5.00	1.00	6.00	3.00	26.00
Median	14.50	20.50	15.00	44.50	54.00
Q3	60.00	83.50	36.00	82.75	71.00
Max	100.00	100.00	100.00	100.00	100.00
Mean	32.36	39.27	26.57	45.89	49.48

The values are explained in Clarke (2017), with 55 as the chromosome size, 0.13 as the mutation rate and 1600 the maximum number of replacements, that terminates the genetic algorithm. None of the calibrations seemed to become stuck at local maxima, in fact the lowest Maximum OSM usually terminated with fewer generations, between 14 and 19, noting that the first iteration is generation "0". Parameters during evolution for subtile ca2dd, with the third quartile Maximum OSM, are shown in Fig. 6. Note the initially assigned values produced a good fit, but during generations 2–10 they underwent considerable change, eventually remaining unchanged from generations 10–19, but with the mean gene fitness slowly rising then falling until the lack of further improvement terminated the sequence.

The OSM of the best performing gene, as stated above, is a composite measure of 8 of the 13 SLEUTH fit parameters. Fig. 7 shows a radar plot of all 13, with the independent goodness of fit measures included for the five subtiles listed in Table 1. All of the individual values are scaled from 0 to 1, and many are r-squared Pearson's correlation coefficients from regressions between values measured from the known calibration maps, and their equivalent values from the model. A perfectly modeled subtile would have values near one for all of the coefficients. All five of the subtiles shown have very low values for at least one of the metrics. Product, Lee-Sallee and Cluster (Mean Cluster Size) seem to be the best discriminators where 'product' is simply the product of the other 12 metrics, so it is not surprising to find its values low; 'Lee-Sallee' is the ratio of the intersection to the union of the urban extents. High values imply a perfect spatial match, which is

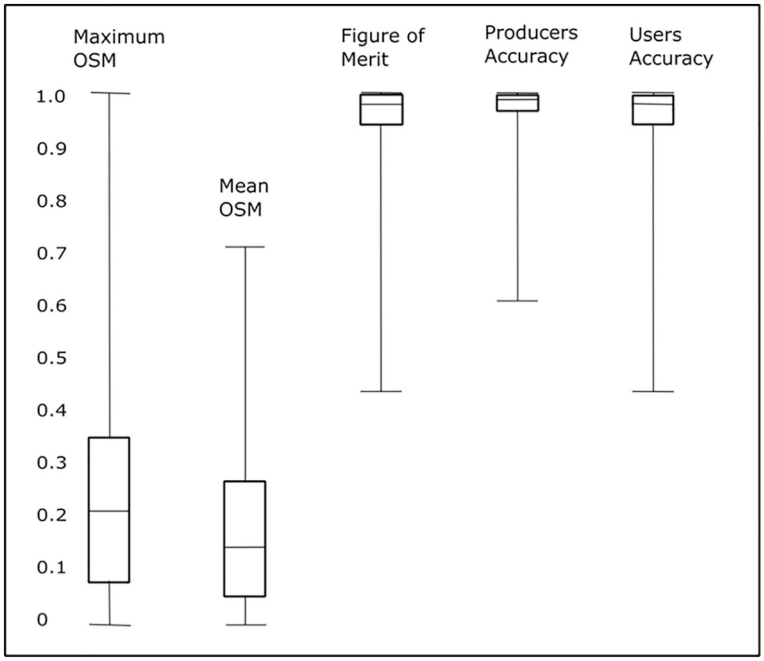

Fig. 3. Boxplot of the SLEUTH performance metrics across the 174 tiles.

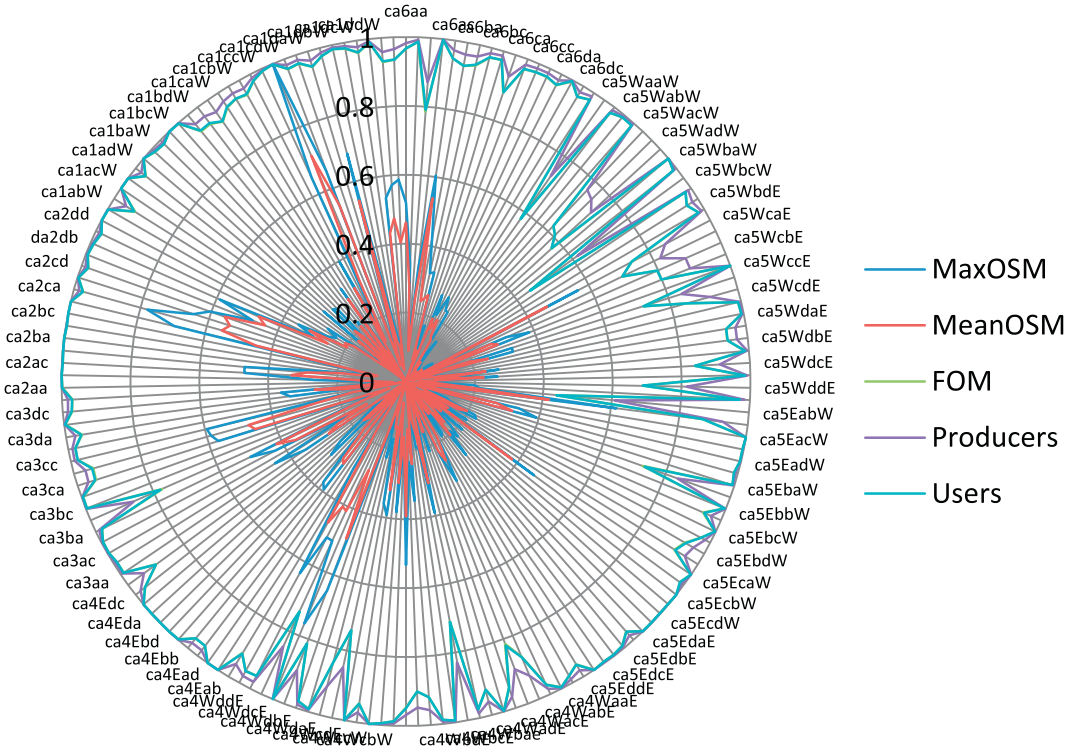

Fig. 4. Radar plot of the five performance metrics by subtile.

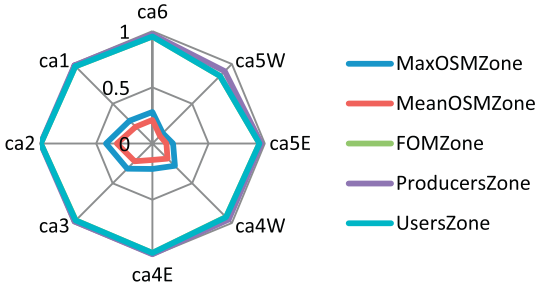

Fig. 5. Radar plot of the five performance metrics by zone.

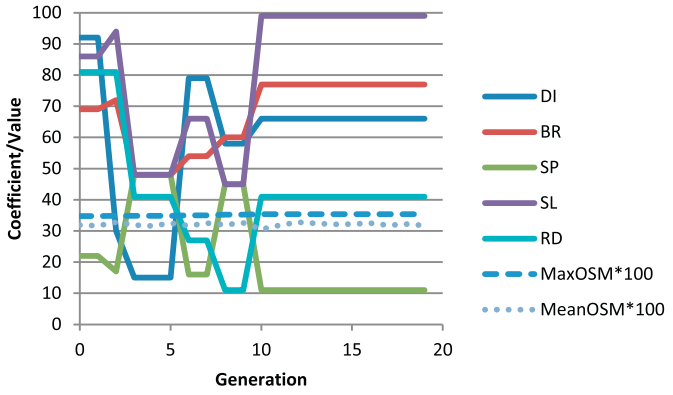

Fig. 6. Change in the coefficient values for the 5 SLEUTH control parameters during calibration by genetic algorithm for subtile ca2dd. Note that the Maximum OSM (best performing gene) and Mean OSM (across the whole chromosome) are multiplied by 100 to be in the same range as the coefficients.

very difficult to accomplish when the growth rate is high and the growth scattered or sprawling. Lastly, the mean cluster size can be highly skewed when one large urban "blob" dominates a set of smaller areas, so this measure is sensitive to getting the urban areas size

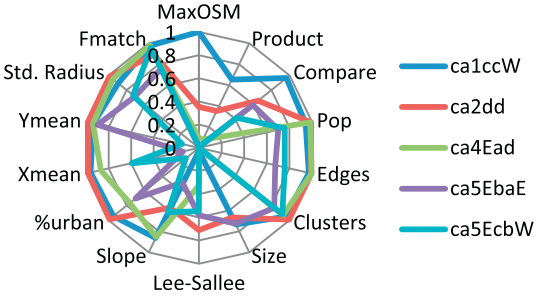

Fig. 7. Radar plot of the 13 SLEUTH degree of fit metrics, plus the Maximum OSM, for the five subtiles listed in Table 1.

distribution correct. However, the five subtiles scored well on many of the OSM measures, especially those reflecting location and distribution.

SLEUTH allows growth to occur as a result of 5 different growth stages. Table 3 contains the ranges and descriptive statistics for the 174 calibrations (aggregated by) subtile for the five behavioral coefficients that control the SLEUTH growth stages. All values are in the range {0…100} as integers. *Diffusion* controls the degree of scatter of newly urbanized cells. At 0, there is no diffusion and all growth takes place as the spread of existing urban cells, while at 100 any non-urbanized cell can be urbanized at random. *Spread* controls the outward spread and infill of urban cells. Zero prevents all spread, while 100 adds outward spread to every urban pixel in the image. *Breed* controls the likelihood of a newly converted, but isolated, urban cell to begin its own growth. At zero, no isolated cells grow, while at 100, all do. *Slope* is a weighted resistance factor that prevents urban cells from growing uphill. Values range from zero, where slope does not matter to growth, to 100 where cells can grow uphill until a maximum slope value (CRITICAL_SLOPE) is reached. For this application, this critical value was 25%, and all slopes greater than this could not be urbanized, although they could change among the other land use classes. Slope also acts in selecting which new land use class is chosen when other classes transition. The *road gravity* coefficient affects the degree to which newly urbanized cells are

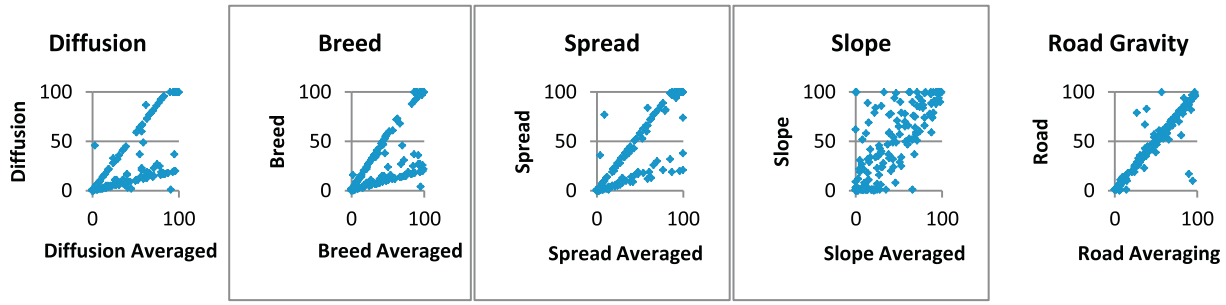

Fig. 8. Scatter plots of the best SLEUTH calibration parameters before and after averaging across 100 Monte Carlo iterations at the start (y) and end (x) of the calibration period.

attracted to and moved along roads. At zero roads have no impact, while at 100 all roads attract all growth within a constant distance. Across the 174 tiles, the values covered the full range for each of the five coefficients, with mean values ranging from 26.57 (Breed) to 49.48 (Road) and the median values ranging from 14.50 (Diffusion) to 54 (Road).

The calibration values that yielded the maximum OSMs were used as input to SLEUTH and run over the calibration period (2001–2017) for 100 Monte Carlo iterations. The ending values of each run were averaged across the 100 runs. This is necessary because the coefficients are changed by reactive self-modification during the run, and prediction needs to start at the end year of the calibration. The big data calibration provided an opportunity to explore how the start and end coefficients are related. Fig. 8 shows the five coefficients, with the values on the y axis being the initial and the x axis being the averaged values. Most fall along the 45 degree line, with values unchanged by periods of boom or bust. Some "max out" and increase to 100 only to remain there. Diffusion, breed and spread often increase by a constant multiplier, the effect of self-modification and an indication that these tiles are in "boom" mode, i.e. are undergoing rapid growth. In a few instances, where points lie above the line, the opposite "bust" has taken place and the values have been reduced. Slope shows the most change, since it is modified both by weighting and reactive self-modification.

To begin to answer the research question regarding spatial autocorrelation, the five behavioral coefficients were averaged by zone. Fig. 9 shows the averages by zone in order as a radar plot. Values seem higher for all parameters except slope in zone ca1 (in the far north) with some significant differences zone to zone. These differences are explored in more detail in the following section.

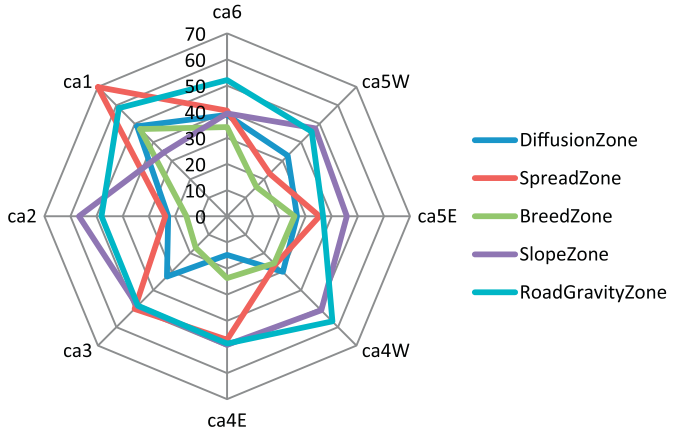

Fig. 9. Radar plot of average SLEUTH coefficients derived from calibration by zone. Values plotted are before averaging.

7. Mapping the calibration

Choropleth maps were prepared by subtile for all of the metrics using R. First, the 5 performance measures were plotted (Fig. 10).

The maximum and mean OSM values showed the most range, and similar spatial distributions with highs in northern California (Zones 1 and 2), and lows in Central California (Zone 5 W). The independent metrics were universally high, with lows in Zone 5 W, but even there interspersed with high values.

Similar maps were prepared for the five best fit SLEUTH coefficients for each subtile. These maps (Fig. 11) show that not only was there great variation across subtiles, there were also similar and opposite values from subtile to subtile. For example, the block of four subtiles in the center/west of Zone 1 had high values for diffusion, spread, breed and road gravity, but low values for slope. There was also evidence of spatial autocorrelation, with values being similar within clusters, and even across zone boundaries.

Fig. 12 shows the coefficients at the end of the calibration period averaged over 100 Monte Carlo iterations. It is noticeable that the averaging seems to diminish the middle ranges for those shown in Fig. 11, and to actually increase the amount of clustering and contrast. Next, to quantify the actual amount of spatial autocorrelation across the two sets of coefficients and five goodness of fit measures, the R software was used to compute the value of Moran's I and its statistical significance (Table 4). Values of I usually range from negative one to positive one. Values significantly below $-1/(N\text{-}1)$ (for California, $N = 174$ so $-1/(N\text{-}1) = -0.00578$) indicate negative spatial autocorrelation, that is, values are dissimilar from their neighbors. Conversely, values significantly above $-1/(N\text{-}1)$ indicate positive spatial autocorrelation. For statistical hypothesis testing, Moran's I values can be transformed to z-scores, and this was used to create the values shown in Table 4, using the 95% significance level.

All of the fit metrics proved significant at the 95% level, with Moran's-I values from 0.237 to 0.282, rejecting the null hypothesis and proving spatial autocorrelation in model fit by subtile. Curiously, none of the initial calibration coefficient values, except spread, showed spatial autocorrelation, but all of the averaged values, except road gravity, did. This implies that just as the GA trains the model, the coefficient values seem to adjust during calibration to reflect the spatial autocorrelation inherent within the input data sets. This furthers the argument in favor of rejecting the null hypothesis.

8. Forecasting with SLEUTH

With the calibration complete, the next stage was to run simulations using the best sets of coefficients for the period 2017–2100. As forecasts, there can be no accuracy measure comparable to the calibration, but the accuracy measures are believed to be indicators of the confidence or reliability of the forecasts. Maps of the actual forecasts are to be published elsewhere. As a simple summary, Table 5 lists the numbers of hectares in each of the 13 land use classes for 2001 and 2100.

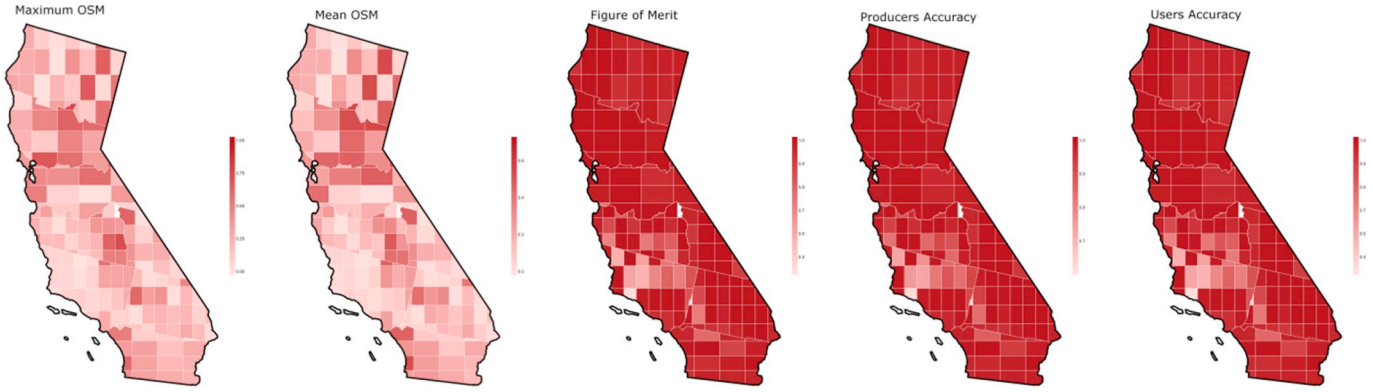

Fig. 10. Performance metrics for the 174 subtiles. White partial subtiles had no change, and therefore no metrics.

Notable is the forecast 162% increase in urban land, from 2,743,179 ha in 2001 to 7,199,339 ha in 2100. In contrast to the rapid growth in San Francisco and Los Angeles and their surrounding suburban areas at the end of the 20th century, coastal California's growth is projected to be minimal, but major urban expansions are expected in the southern San Joaquin Valley, north of the Salton Sea, and around Interstate 10 near Indio and Palm Springs. Other expansion is in the valleys of the Sierras, around Bishop and in the valleys of the Sierra Nevada Mountains in Modoc, Lassen and Plumas Counties. Evergreen forest and shrubland are expected to increase in area in addition to urban, and agricultural land and grassland areas are expected to decrease in area.

SLEUTH contains options for labeling pixels that are converted to urban with the behavioral rule that triggered their change. The projections allowed a closer examination of how and where the four CA rules expanded urban areas. The four rules that led to urbanization were dominated by the spread rule, with 98.8% (36,337,322 cells) of the conversions triggered by this rule that simply adds pixels to existing clusters of urban pixels. Diffusion, in which pixels detached from currently urban areas become urban, accounted for 0.66% (242,935 cells) of the urban growth, while the breed rule accounted for 0.47% (173,658 cells). The combination of diffusion and breed is how new spreading centers form, and while they are few in number, they create important changes in the urban form. Lastly, the road growth rule draws newly urbanized cells toward roads, and creates new settlements along those roads. Road growth accounted for only 0.08% of the growth (29,626 cells). The actions of these rules are evident in Fig. 13, which shows enlargements of areas within zone 6. In the upper left panel of Fig. 13, an area with many existing roads attracted road growth (cyan) that was later expanded through spread (blue). The upper right panel shows examples of new settlements, created initially by the diffusion rule (green) then expanded by the breed rule (yellow) so that subsequent growth took place according to the spread (blue) rule. The lower left panel shows examples of both existing urban pixels and two diffusion rule pixels (green), one of which started to grow due to the breed (yellow) and spread (blue) sequence, and one that failed to do so, while two existing isolated urban pixels failed to grow at all.

Although the new urban growth was largely due to the spread rule, maps of the numbers of new urban pixels by subtile are shown in Fig. 14. Sheer numbers of pixels show some consistency, with a clear link between diffusion, spread and breed rules spatial distribution, again showing a high hot spot in zone 5 W. Values are generally high in the east of Zone 1, but especially so for the road trip rule. Attraction to existing roads seems to have a major influence on the expected high rate of urban spread in this region. The right-most map in Fig. 14 shows percent growth by subtile, a value that ranges from 0.0% to 932.7%, with a mean of 180.1% and a median of a 49.1% increase. The highest growth rates correspond with the highest number of growth pixels, but also with the parameter distributions shown in Fig. 12. These maps were also tested for spatial autocorrelation using Moran's *I*, with the results shown in Table 6. All showed strong autocorrelation, with the highest value (0.7740) being the existing (2017) number of urban pixels. The growth rate (0.4820) and the diffusion rule (0.4270) are also very highly spatially autocorrelated. This again lends strength to the rejection of the null hypotheses of no spatial autocorrelation in the model forecasts, in addition to the model calibration.

In summary, both the SLEUTH calibration and forecasts showed significant spatial autocorrelation and ranges of values across the state of California. Calibration fit ranged from very low to very high, but in most cases skewed toward high. This implies that a lack of growth, just like very rapid growth, has unique causal factors and locations that are

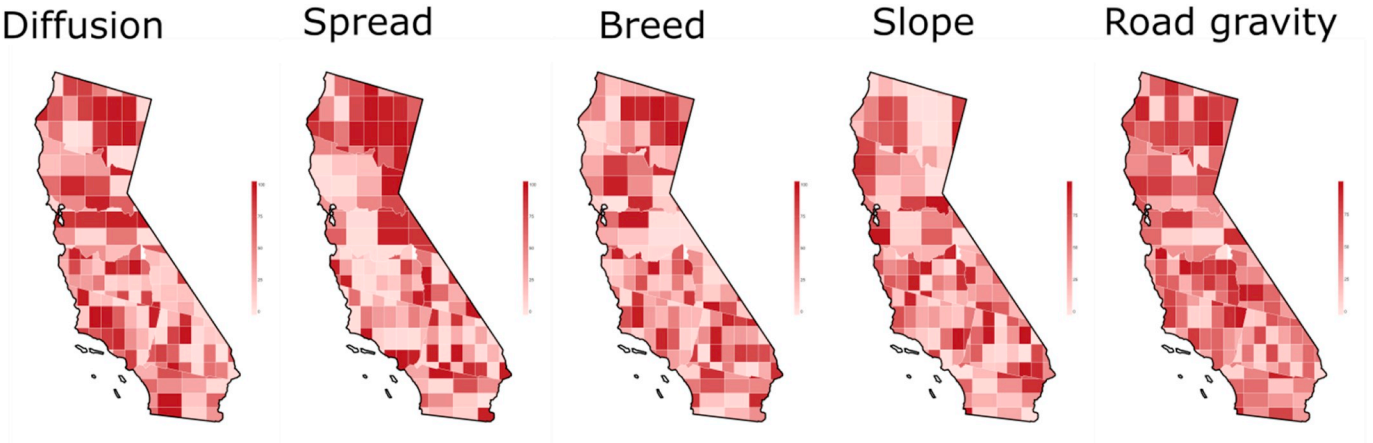

Fig. 11. Best fit SLEUTH coefficients from the initial calibration for California mapped by subtile.

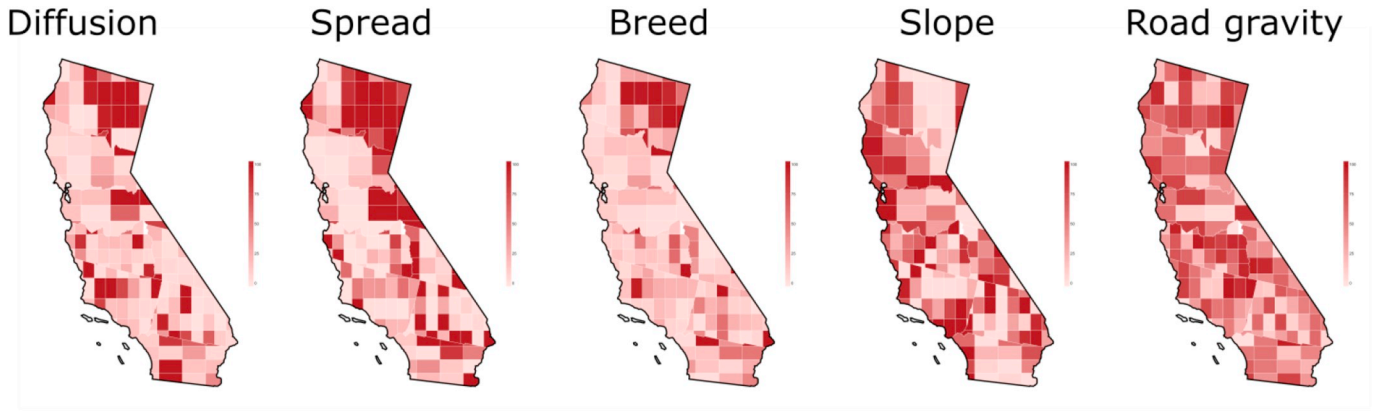

Fig. 12. Best fit SLEUTH coefficients from calibration averaged for 2017 over 100 Monte Carlo iterations for California mapped by subtile.

Table 4
Moran's I values for each of the fit and coefficient measures for the SLEUTH calibration.

Name	p_value	Moran's-I	Sig. (5%)
MaxOSM	0.001	0.2820	TRUE
MeanOSM	0.001	0.2800	TRUE
FOM	0.001	0.2490	TRUE
Producers Accuracy	0.001	0.2370	TRUE
Users Accuracy	0.001	0.2520	TRUE
Diffusion - Calibration	0.192	0.0320	FALSE
Spread - Calibration	0.001	0.2200	TRUE
Breed - Calibration	0.303	0.0170	FALSE
Slope - Calibration	0.291	0.0170	FALSE
Road Gravity - Calibration	0.457	−0.0040	FALSE
Diffusion- Averaged	0.004	0.1150	TRUE
Spread -Averaged	0.001	0.2430	TRUE
Breed -Averaged	0.001	0.2030	TRUE
Slope-Averaged	0.004	0.1170	TRUE
Road Gravity-Averaged	0.293	0.0160	FALSE

captured by the model, and that the effect of these extrema is to influence adjacent subtiles and areas. This is a strong effect and was proven to be significant for most of the fitness metrics, for the model calibration parameters and for the amounts of simulated growth.

9. Uncertainty in the calibrations and forecast

There are three sources of uncertainty in the SLEUTH modeling effort: the data, the calibration and the forecasts. The MRLC land use data are based on Landsat satellite and other data, and the extraction of classified land use from such data is known to be imperfect for reasons of the vagueness in class descriptions, imprecision in class semantics and other inaccuracy in the classification process. That said, Wickham et al. (2017) found that the MRLC single-date overall accuracies were 82%, 83%, and 83% at Level II and 88%, 89%, and 89% at Level I for 2011, 2006, and 2001, respectively.

Unfortunately, at the time this project began, the NLCD land cover only extended to 2011. However, the USDA products offered geospatial estimates of urban areas out to 2017. To maximize the use of both of these datasets it was assumed that landcover did not change between 2011 and 2017. The net effect may be to underestimate change in the modeling. SLEUTH is known to be sensitive to pixels that change out of the urban class, so by forward overlay processing, any urban pixel was changed to urban for all subsequent years. The impact could be overestimation, especially where settlements are losing population. Lastly, while every effort was made to preserve the land geometry nevertheless some of the data, especially the roads, showed slight displacements over time, which can lead to false transitions. Finally, the weights in the exclusion layer were assigned by judgement and consensus, but nevertheless were subjective and liable to error. Liu et al. (2019) concluded that using exclusion layers without effective limits in SLEUTH might result in unreasonable prediction of future built-up land.

Secondly the model calibration itself introduced possible errors. SLEUTH calibration revealed results that showed unexpectedly large variations of both the behavioral coefficients and the degree of fit across subtiles and zones. No attempt was made to eliminate or smooth out these differences, and as a result the tile and zone boundaries are in some cases visible in the forecasts. Leaving these obvious errors in place was more honest than attempting to smooth them out. The SLEUTH data processing and the calibration were user and CPU time intensive. Several small C language scripts were written to adjust color tables, conflate images, divide data tiles, and reassemble the final maps. In some cases, calibrations were repeated when the results were doubted, with some entire zones going through the calibration process three times.

Table 5
Past and Projected Land Use Change in California 2001–2100 using the SLEUTH modeling described.

Land Use	Hectares (2001)	Percent (2001)	Hectares (2100)	Percent (2100)	Change Ha (2001 − 2100)	PERCENT Change (2001–2100)
Urban	2,743,179	6.69	7,199,339	17.56	4456,160	162.45
Water	620,477	1.51	605,587	1.48	−14,890	−2.40
Permanent Ice & Snow	4075	0.01	2494	0.01	−1581	−38.81
Barren	1,996,573	4.87	1,656,437	4.04	−340,136	−17.04
Dec. Forest	354,241	0.86	217,402	0.53	−136,839	−38.63
Evergreen Forest	8,349,849	20.37	8,242,761	20.10	−107,088	−1.28
Mixed Forest	1,013,537	2.47	793,222	1.93	−220,314	−21.74
Shrubland	16,232,513	39.59	15,185,704	37.03	−1,046,809	−6.45
Grassland	5,237,890	12.78	4,080,716	9.95	−1,157,173	−22.09
Pasture	766,215	1.87	485,422	1.18	−280,793	−36.65
Orchards/Row Crops	3,354,812	8.18	2,288,693	5.58	−1,066,119	−31.78
Woody Wetland	100,131	0.24	60,553	0.15	−39,577	−39.53
Herbaceous Wetland	224,702	0.55	186,564	0.45	−38,138	−16.97

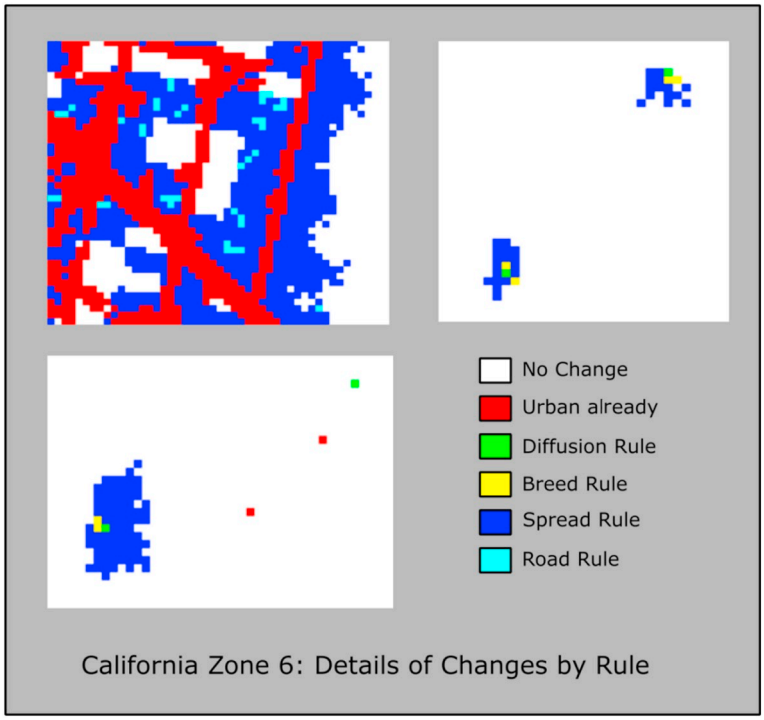

Fig. 13. Details from subtiles in California zone 6 showing urban conversion by the CA rule that led to the change.

The use of the genetic algorithm for calibration reduced the CPU time and human control necessary. However, a genetic algorithm itself requires calibration, and the values used were those researched in Clarke (2017), with a chromosome of 55 genes, and a mutation rate of 0.13. The maximum number of replacements of genes, which controls the time of calibration and the number of generations was set at 1600, which gave a consistent completion of the evolution at 20 generations, with very few exceptions. Other variations in the performance and coefficients in the calibration were the subject of the current research.

Lastly, SLEUTH forecasting involves uncertainty. SLEUTH tracks forecast uncertainty by creating maps of two kinds. First, over the 100 Monte Carlo iterations for the prediction, a count is made of how many times each pixel became urban, and these yield expected probabilities of urbanization. Secondly, once a simulation is complete and a final land use chosen, a specific land use class is chosen by voting across the 100 iterations. A pixel that is assigned a new land use of the same type in all 100 iterations is assigned 0 uncertainty. A pixel is assigned the majority class, but sometimes this value can fall lower, for example a pixel could theoretically be assigned equally to all 13 classes with 1/13 = 7.7% probability, with a selected class being assigned that high value of uncertainty (100–7.7 = 92.3% uncertain). These two uncertainty values were mapped and are shown in Fig. 15 for the Paso

Table 6
Moran's I calculations for the growth rule variables shown in Fig. 12.

Name	p_value	Moran's-I	Sig (5%)
Number of Pixels Urban in 2017	0.001	0.7740	TRUE
Pixels by Diffusion Growth	0.004	0.4270	TRUE
Pixels by Breed Growth	0.001	0.1120	TRUE
Pixels by Spread Growth	0.003	0.1850	TRUE
Pixels by Road Growth	0.001	0.1330	TRUE
Percent Growth2017–2100	0.001	0.4820	TRUE

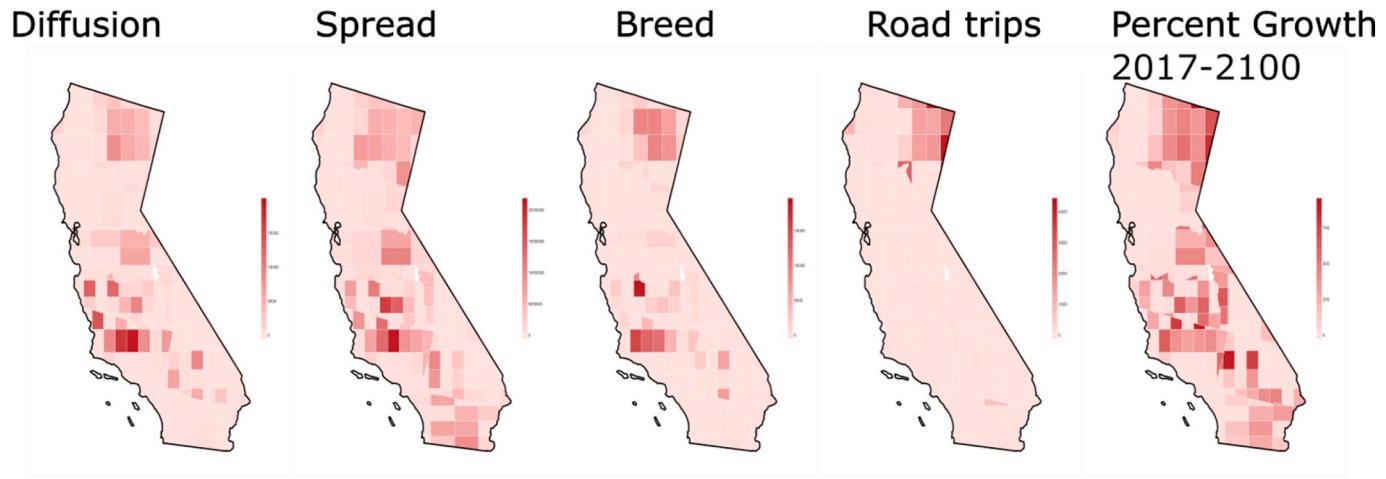

Fig. 14. Counts of the number of pixels converted to urban during the 2017–2100 simulation by each of the four CA behavior rules. Far right map is for the total urban growth rate by cells in percent. Note that the scales vary by behavior rule.

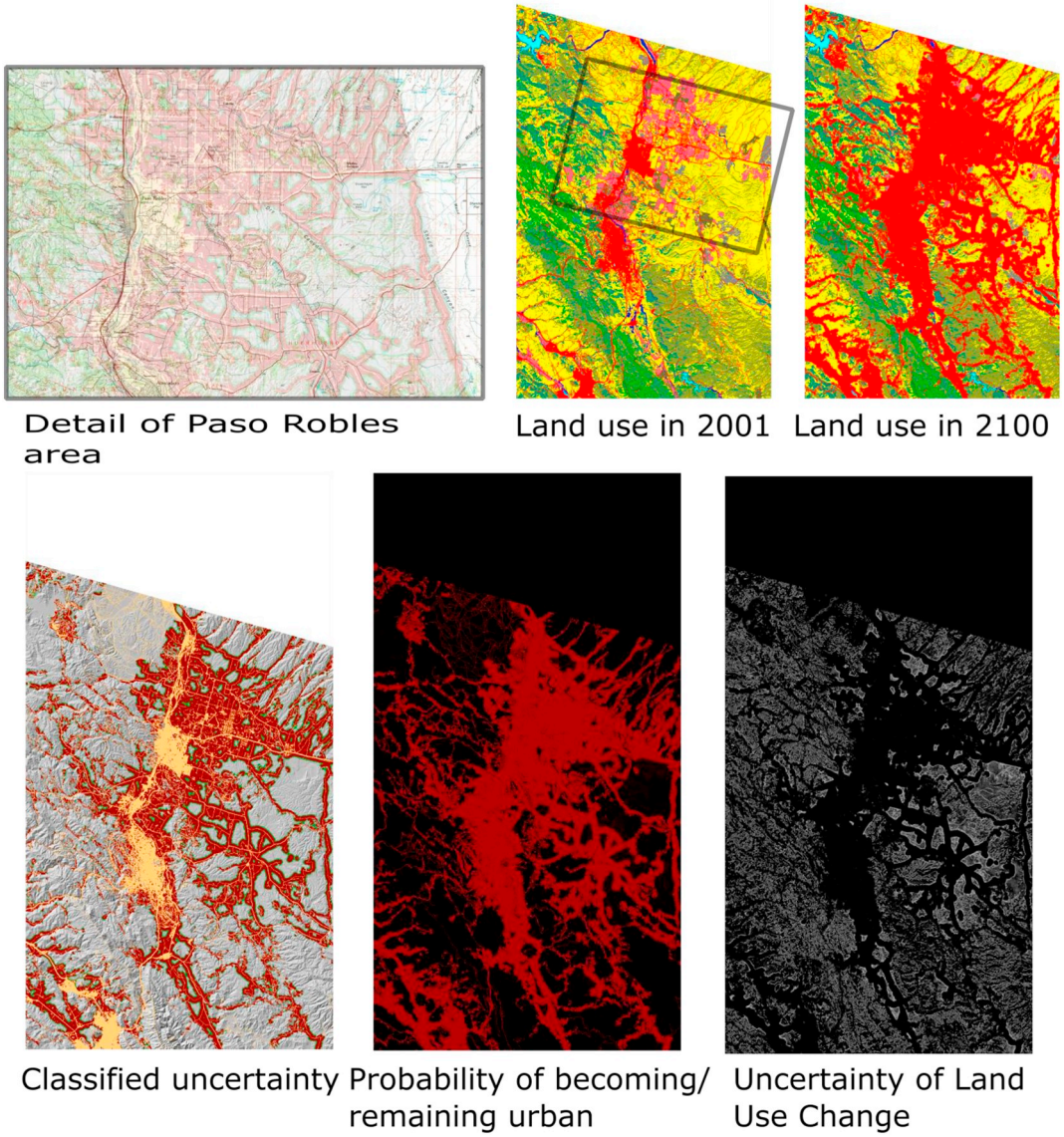

Fig. 15. Uncertainty maps for Paso Robles/Atascadero area surrounding Highway 101 in California in subtile ca5WaaW. Upper left; Detail showing topographic map. Upper Right: Land use maps in 2001 and 2100, class colors Red = Urban; Pink = Agriculture; Green = Forest and Rangeland. Lower left: Uncertainty classified: Yellow = urban in 2017; Red = 95–100% certainty of urban in 2100;Green = 50–94% certainty of urban in 2100. Lower center: Monte Carlo likelihood of being urban in 2100. Lower right: Grey scale level of uncertainty of land use class label for all classes. (For interpretation of the references to color in this figure legend, the reader is referred to the web version of this article.)

Robles area in San Luis Obispo County While their Moran's-I values were not computed, the maps reveal strong spatial autocorrelation.

Lastly it is worth noting that SLEUTH does not account for population. If, for example, California's high cost of living causes an exodus of people then the forecasted growth may not come to fruition as there is not the population to demand it. Further changes in demographic structure, changes in conservation priorities, or social changes such as a preference for dense urban living (smart growth) are not modeled. Neither have we attempted to compare our modeling forecasts with those of other studies (e.g. Sleeter, Wilson, Sharygin, & Sherba, 2017).

10. Big data and SLEUTH

Lessons were learned through having to deal with massive amounts of data in SLEUTH modeling. Three keys to bulk data processing were: (1) tiling the data into manageable chunks that allowed each subtile to be calibrated (and forecast) largely independently; (2) simplification of the number of data layers and the use of the genetic algorithm made the model application tractable in terms of CPU time; and (3) the tile naming convention made it possible to repeatedly use the same scenario files and shell scripts with only minor changes from run to run. This reduced user time, and allowed rapid viewing and repetition of tile calibrations when necessary.

It was still necessary to handle the data in bulk, by zone and entire state, and for this purpose a GIS (ArcGIS10.3) was used. Intermediate visualization made extensive use of the open source tool GIMP, which has remarkable format flexibility. Lastly, file sizes were kept under control by using two forms of the Graphics Interchange Format (GIF), that can be either grayscale or indexed color.

Perhaps the most important lessons learned by using SLEUTH with big data were first, that very high resolutions made it feasible to look up exact locations on web mapping systems to see whether the model results made sense, and second, that more aggregate modeling averages out immense local variations in both model fit and the best model coefficients. While in general the model performed extremely well, application at a coarser scale would miss much of the richness of detail

now possible by high resolution modeling.

11. Conclusion

This study set out to investigate whether spatial autocorrelation exists among SLEUTH calibrations when massive data sets are spatially tiled to make computations possible. Data for the state of California on land use and other factors was used at a 30 m resolution, which required divisions into State Plane zones, then tiles and in most cases subtiles. Of the 192 subtiles, only 174 contained data for calibration. SLEUTH was calibrated for these subtiles using repeated changes to scenario files containing file names and other data. A genetic algorithm reduced the necessary computation time to about a year of CPU time across two different computers. Across the 174 subtiles, the five calibrated coefficients covered the full range from zero to 100, the means ranged from 26.57 (Breed) to 49.48 (Road) while the medians ranged from 14.50 (Diffusion) to 54 (Road). Spatial autocorrelation was proven with 95% confidence for not only the performance and accuracy metrics, but also for the five calibration coefficients. Once calibrated, SLEUTH was used to forecast California land use from 2017 to 2100, for an estimated 162% increase in urban land by the end of the 21st century, with 98.8% of the growth caused by outward spread of existing (and some new) settlements. Given the uneven spatial pattern of the model's coefficients, their spatial autocorrelation then propagated into the forecasts based on these coefficients to produce behavior that was also spatially autocorrelated, best illustrated by the high degree of clustering in high values of the road gravity coefficients. The uncertainty associated with the projections was estimated using Monte Carlo methods, and mapped for the expected land use future.

A growth in urban land use by 2100 of 4,456,160 ha alone is a sobering prospect for the state. However, other changes such as the loss of farmland and wildlands are also challenges. California's future residents will increasingly live in areas that are prone to earthquakes, wildfire, drought and climate changes, such as sea level rise and higher temperatures. With the state population at almost 40 million today, continued economic and population growth and an abundance of land available for development, SLEUTH's forecasts are within the limits of feasibility. Local and patchwork growth management strategies or their absence may be among the causes of the great range in forecast growth rates from 0.0% to 932.7% by subtile, with a mean of 180.1% and a median of 49.1% increase. A more sustainable land use future may require coordinated statewide growth planning, and the adoption of smart growth principles in planning to deal with this highly varied, but highly autocorrelated future growth and change.

References

Akin, A., Clarke, K. C., & Berberoglu, S. (2014). The impact of historical exclusion on the calibration of the SLEUTH urban growth model. *International Journal of Applied Earth Observation and Geoinformation, 27*(B), 156–168.

CAGIS (Center for Applied Geographic Information Science) (2019). SLEUTH3R (Smart SLEUTH). https://gis.uncc.edu/products/smart-sleuth.

Chaudhuri, G., & Clarke, K. C. (2013). The SLEUTH land use change model: A review. *International Journal of Environmental Resources Research, 1*(1), 88–104.

Chaudhuri, G., & Foley, S. (2019). DSLEUTH: a distributed version of SLEUTH urban growth model. *ANSS '19 Proceedings of the annual simulation symposium, 15. Tucson, AZ — April 29 - May 02, 2019.* San Diego, CA: Society for Computer Simulation International.

Clarke, K. (2017). Improving SLEUTH calibration with a genetic algorithm. *Proceedings of the 3rd international conference on geographical information systems theory, applications and management (GISTAM 2017)* (pp. 319–326). (ISBN: 978-989-758-252-3).

Clarke, K. C. (2008). In R. K. Brail (Ed.). *A decade of cellular urban modeling with SLEUTH: Unresolved issues and problems, Ch. 3 in planning support systems for cities and regions* (pp. 47–60). Cambridge, MA: Lincoln Institute of Land Policy.

Clarke, K. C. (2018). Land use change Modeling with SLEUTH: Improving calibration with a genetic algorithm. Chapter 8 (pp. 139-162). In M. T. C. in Olmedo, M. Paegelow, J.-P. Mas, & F. Escobar (Eds.). *Lecture Notes in Geoinformation and Cartography*. (pp. 521–525). Springer. https://doi.org/10.1007/978–3–319-60801-3_39.

Clarke, K. C. (2019). Mathematical foundations of cellular automata and complexity theory. In L. D'Acci (Ed.). *The mathematics of urban morphology, modeling and simulation in science, engineering and technology* (pp. 163–172). Birkhauser: Springer Nature.

Clarke, K. C., Hoppen, S., & Gaydos, L. (1996). Methods and techniques for rigorous calibration of a cellular automaton model of urban growth. *Proceedings, third international conference/workshop on integrating geographic information systems and environmental modeling, January 21- 25th, Santa Fe, NM*.

Clarke-Lauer, M. D., & Clarke, K. C. (2011). Evolving simulation modeling: Calibrating SLEUTH using a genetic algorithm. *Proceedings., 11th international conference on geo computation, Univ. College London, London*. Online at www.geog.leeds.ac.uk/groups/geocomp/2011/papers/clarke-lauer.pdf.

Dietzel, C., & Clarke, K. C. (2005). The effects of disaggregating land use categories in cellular automata during model calibration and forecasting. *Computers, Environment and Urban Systems, 30*(1), 78–101.

Dietzel, C., & Clarke, K. C. (2007). Toward optimal calibration of the SLEUTH land use change model. *Transactions in GIS, 11*(1), 29–45.

Foley, J. A., DeFries, R., Asner, G. P., Barford, C., et al. (2005). Global consequences of land use. *Science, 309*(5734), 570–574.

Goldstein, N., Dietzel, C., & Clarke, K. (2005). *Don't stop 'Til you get enough - sensitivity testing of Monte Carlo iterations for model calibration in Yichun Xie and Daniel G. Brown.* GeoComputation CD-ROMhttp://www.geocomputation.org/2005/index.html.

Guan, Q., & Clarke, K. C. (2010). A general-purpose parallel raster processing programming library test application using a geographic cellular automata model. *International Journal of Geographical Information Science, 24*(5), 695–722.

Herold, M., Couclelis, H., & Clarke, K. C. (2005). The role of spatial metrics in the analysis and Modeling of urban land use change. *Computers, Environment and Urban Systems, 29*, 369–399.

Houet, T., Aguejdad, R., Doukari, O., Battaia, G., & Clarke, K. (2016). Description and validation of a 'non path-dependent' model for projecting contrasting urban growth futures. *Cybergeo European Journal of Geography, Systèmes, Modélisation, Géostatistiques*. https://doi.org/10.4000/cybergeo.27397 document 759.

Jafarnezhad, J., Salmanmahiny, A., & Sakieh, Y. (2015). Subjectivity versus objectivity: Comparative study between brute force method and genetic algorithm for calibrating the SLEUTH urban growth model. *Urban Planning & Development.*. https://doi.org/10.1061/(ASCE)UP.1943-5444.0000307.

Jantz, C., Drzyzga, S., & Maret, M. (2014). Calibrating and validating a simulation model to identify drivers of urban land cover change in the Baltimore, MD metropolitan region. *Land, 3*, 1158–1179. https://doi.org/10.3390/land3031158.

Jantz, C. A., & Goetz, S. G. (2005). Analysis of scale dependencies in an urban land-use-change model. *International Journal of Geographical Information Science, 19*(2), 217–241. https://doi.org/10.1080/13658810410001713425.

Jantz, C. A., Goetz, S. J., Donato, D., & Claggett, P. (2010). Designing and implementing a regional urban modeling system using the SLEUTH cellular urban model. *Computers, Environment and Urban Systems, 34*, 1–16. https://doi.org/10.1016/j.compenvurbsys.2009.

Liu, X., Sun, R., Yang, Q., Su, G., & Qi, W. (2012). Simulating urban expansion using an improved SLEUTH model. *Journal of Applied Remote Sensing, 6*(1), https://doi.org/10.1117/1.JRS.6.061709.

Liu, Y., Li, L., Cheng, L., Zhou, X., Cui, Y., Li, H., & Liu, W. (2019). Urban growth simulation in different scenarios using the SLEUTH model: A case study of Hefei, East China. *PLoS One, 14*(11), Article e0224998. https://doi.org/10.1371/journal.pone.0224998.

Martellozzo, F., Amato, F., Murgante, B., & Clarke, K. C. (2018). Modelling the impact of urban growth on agriculture and natural land in Italy to 2030. *Applied Geography, 91*, 156–160.

Oak Ridge National Laboratory (2020). Landscan datasets (nd) https://landscan.ornl.gov/landscan-datasets.

Onsted, J., & Clarke, K. (2012). The inclusion of differentially assessed lands in urban growth model calibration: A comparison of two approaches using SLEUTH. *International Journal of GIS, 26*(5), 1–18.

Peiman, R., & Clarke, K. C. (2014). The impact of data time span on forecast accuracy through calibrating the SLEUTH urban growth model. *International Journal of Applied Geospatial Research, 5*(3), 21–35.

Pontius, R. G., Jr., Boersma, W., Castella, J.-C., Clarke, K., de Nijs, T., Dietzel, C., ... Verburg, P. H. (2007). Comparing the input, output, and validation maps for several models of land change. *Annals of Regional Science, 42*(1), 11–37.

Sakieh, Y., Salmanmahiny, A., & Mirkarimi, S. H. (2016). Rules versus layers: Which side wins the battle of model calibration? *Environmental Monitoring and Assessment, 188*(11), 1–26. https://doi.org/10.1007/s10661-016-5643-2.

Saxena, A., & Jat, M. K. (2018). Analysing performance of SLEUTH model calibration using brute force and genetic algorithm–based methods. *Geocarto International*. https://doi.org/10.1080/10106049.2018.1516242.

Silva, E. A., & Clarke, K. C. (2002). Calibration of the SLEUTH urban growth model for Lisbon and Porto, Portugal. *Computers, Environment and Urban Systems, 26*(6), 525–552.

Sleeter, B. M., Wilson, T. S., Sharygin, E., & Sherba, J. S. (2017). Future scenarios of land change based on empirical data and demographic trends. *Earth's Future, 5*, 1068–1083. https://doi.org/10.1002/2017EF000560.

Wickham, J., Stehman, S. V., Gass, L., Dewitz, J. A., Sorenson, D. G., Granneman, B. J., ... Baer, L. A. (2017). Thematic accuracy assessment of the 2011 National Land Cover Database (NLCD). *Remote Sensing of Environment, 191*, 328–341. https://doi.org/10.1016/j.rse.2016.12.026.

Wu, X., Hu, Y., He, H. S., Bu, R., Onsted, J., & Xi, F. (2009). Performance evaluation of the SLEUTH model in the Shenyang metropolitan area of Northeastern China. *Environmental Modeling & Assessment, 14*(2), 221–230. https://doi.org/10.1007/s10666-008-9154-6.

Zhou, Y., Varquez, A. C. G., & Kanda, M. (2019). High-resolution global urban growth projection based on multiple applications of the SLEUTH urban growth model. *Nature: Scientific Data, 6*, 34. https://doi.org/10.1038/s41597-019-0048-z.